Journal of Korea Robotics Society (2026) 21(2):212-223
212 https://doi.org/10.7746/jkros.2026.21.2.212 ISSN: 1975-6291 / eISSN: 2287-3961

양손 작업이 가능한 두 손가락 엔드 이펙터의 설계와 실험적 검증

Design and Experimental Validation of a Two-Finger End-Effector Capable of Bimanual Manipulation Tasks

강 효 재[1] · 김 희 준[2] · 강 민 성[†]
HyoJae Kang[1], HeeJun Kim[2], Min-Sung Kang[†]

Abstract: This study introduces a new type of two-finger end-effector designed to enable a single robotic manipulator to perform manipulation tasks that typically require two arms. The main objective is to enhance efficiency in both workspace usage and system cost by allowing complex, bimanual manipulation tasks through one manipulator. The system comprises two fingers, where one finger features three serially connected rotational joints and an integrated parallel gripper at its tip. The geometric and kinematic characteristics of the mechanism were analyzed to estimate its reachable workspace. A series of bimanual manipulation experiments were then conducted to evaluate its functional performance and practical applicability. Through experimental validation, it was observed that the proposed mechanism successfully executed various bimanual manipulation tasks that conventionally require coordinated actions of two manipulators. These results demonstrate that cooperative manipulation can be realized by a single arm when equipped with the proposed end-effector. In contrast to prior works focusing mainly on replicating the human hand structure or maximizing degrees of freedom, this study presents a hybrid mechanism that embeds a parallel gripper within a multi-joint finger. The design concept enables compact, efficient manipulation and suggests a simplified yet versatile approach for future robotic systems.

Keywords: End-Effector, Robot Mechanism, Bimanual Manipulation, Parallel Gripper

1. Introduction

The gripper is mounted at the end of a manipulator and is responsible for grasping and manipulating objects. Grippers can be classified according to their mechanisms or applications, including pneumatic grippers[1], hydraulic-powered grippers[2], electric grippers[3], magnetic grippers[4], vacuum grippers[5], and passive grippers[6]. Among these, electric grippers are commonly used in applications requiring precise control. Electric grippers range from simple two-finger parallel types[7,8] to multi-finger grippers[9,10] and dexterous hands[11] that provide human-like degrees of freedom.

To replicate the functionality of the human hand, extensive research has focused on the development of dexterous robotic hands[12-14]. These hands, characterized by a high number of degrees of freedom (DoF), are capable of producing a wide variety of motions and postures, thereby offering broad applicability across diverse domains. However, the high DoF inherent in such designs introduces challenges, including an increased number of actuators, complex control architectures, and elevated

Received : Dec. 19. 2025; Revised : Jan. 24. 2026; Accepted : Mar. 3. 2026
※ This work was supported by the Technology Innovation Program (RS-2024-00442513, Development of robotic manipulation task learning based on foundation model to understand and reason about task situations) funded by the Ministry of Trade Industry Energy (MOTIE, Korea).
1. Graduate Student, Department of Interdisciplinary Robot Engineering System, Hanyang University, Ansan, Korea (majaae5@hanyang.ac.kr)
2. Undergraduate Student, School of Smart Convergence Engineering, Hanyang University, Ansan, Korea (heejun@hanyang.ac.kr)
† Associate Professor, Corresponding author: School of Smart Convergence Engineering, Hanyang University, Ansan, Korea (wowmecha@hanyang.ac.kr)

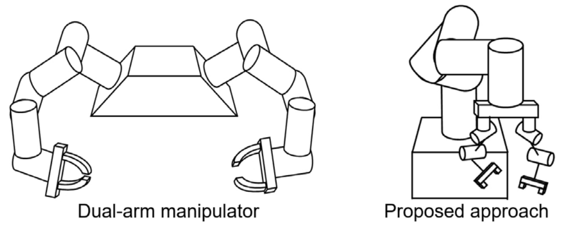

[Fig. 1] Approaches to bimanual manipulation: dual-arm manipulator versus the proposed single-manipulator end-effector

system costs[15,16]. To address these issues, underactuated mechanisms have been widely investigated. The principal advantage of this approach lies in its ability to achieve versatile motion while reducing the number of actuators required for control[17].

Conventional grippers have primarily focused on grasping tasks, whereas robotic hands have been designed to perform both grasping and in-hand manipulation. Traditional in-hand manipu lation mainly involves manipulating an object within a single hand, with a primary focus on changing the object's orientation[18-21]. Such studies have laid the foundation for more sophisticated manipulation strategies that enable precise reorientation and repositioning without external assistance. However, single-hand manipulation becomes limited when tasks require coordinated motion or force interaction between both hands, such as unscrewing a bottle cap or tearing open a plastic package.

To address such tasks, bimanual manipulation has been investigated, as it requires precise motion control and intricate coordination between the two arms[22]. To achieve human-level bimanual manipulation, alternative approaches such as reinforcement learning (RL) have been explored[23]. Studies have shown that imitation learning enhances robotic dual-arm coordination by combining waypoint guidance, hierarchical learning, and force-based control[24-26]. In particular, these systems[26-28] have demonstrated remarkable performance in developing data collection frameworks for imitation learning. Reinforcement learning often suffers from low sample efficiency and training instability, while imitation learning remains labor-intensive and time-consuming due to the need for extensive demonstrations[29]. To overcome these limitations, recent studies have explored high-level planning approaches that leverage large language models (LLMs)[30], vision-language models (VLMs)[31], and vision-language-action (VLA) frame works[32].

Nevertheless, from the perspective of physical interaction, these approaches still rely on two independent grippers operating in parallel. For tasks that do not require high grasping forces, the use of two manipulators tends to be inefficient in terms of both cost and spatial requirements.

Therefore, this study proposes an end-effector designed to enable a single manipulator to perform tasks that typically require dual-arm coordination. As shown in [Fig. 1], the proposed mechanism consists of two fingers, including a three joint articulated finger with an integrated parallel-gripper-like sub-gripper at the fingertip. This configuration allows a single tool to emulate coordinated dual-gripper behavior, enabling precise in-hand manipulation and repositioning of small objects without the complexity of a multi-arm system.

The scope and contributions of this study are summarized as follows:

1. This study proposes an end-effector that enables bimanipulation tasks using a single manipulator, focusing solely on its mechanical design and functional capability.
2. The research emphasizes structural design approaches and experimentally verifies the bimanipulation performance of the proposed mechanism.
3. The applicability of the mechanism is demonstrated through several manipulation scenarios, showing its ability to perform various bimanipulation-like operations.

The following section provides a brief overview of previous studies related to finger design. Section 3 describes the hardware design of the proposed system and kinematic analysis. Section 4 details the experiments and the results obtained from the selected tasks. Section 5 discusses the limitations of the study and outlines directions for future research, while Section 6 concludes the paper.

2. Related Works

Existing research has focused on replicating finger structures analogous to the human hand in order to enable both grasping and in-hand manipulation. This bio-inspired approach aims to mechanically reproduce the biomechanical features of the human hand to achieve flexible and adaptive manipulation. Typically, robotic fingers are classified as either fully actuated[14] or under-actuated[17], each approach representing a trade-off between actuation efficiency and control precision. In a fully actuated design, every joint can be controlled independently, enabling fine motion execution, but this demands complex control architectures and a large number of actuators. Conversely, underactuated designs generate multi DoF motion with fewer actuators, which affords structural simplicity and reduced mass, yet they impose limitations on fine manipulation and force control.

Previous works commonly apply the same structure from the little finger through the index finger, while designing the thumb separately. Most fingers are configured with 2 DoF[17], 3 DoF [33-35], or 4 DoF[14,36], whereas the thumb has been designed with 3 DoF[17], 4 DoF[14,33-35], or 5 DoF[36]. These configurations aim to realize a variety of grasp postures and enable thumb opposition. Moreover, the majority of the prior work addressed structural designs for reliably grasping objects of varying shapes. In particular, adaptive grasping mechanisms-where fingers automatically conform to object geometry-have been actively studied. However, those approaches generally focus on static grasping rather than the dynamic reorientation or repositioning of objects within the hand, i.e., in-hand manipulation. Executing in-hand manipulation requires fine torque control among joints and coordinated kinematics, which is difficult to achieve without advanced control systems. Furthemore, many complex tasks such as assembly or tool usage inherently require two-hand coordination, so many existing systems rely on dual-manipulator setups. Such dual-arm configurations are inefficient in terms of spatial footprint and economic cost, and synchronization control between the arms further adds complexity.

Therefore, although prior works have explored multi-joint robotic hands, adaptive mechanisms, and dual-arm coordination, achieving dual-arm-level dexterous manipulation with a single manipulator remains challenging. This motivates the development of a mechanism that can provide fine manipulation capability without relying on dual-arm control or complex motion planning.

3. Design and Kinematic analysis

3.1 Design of the end-effector

The objective of this study is to enable bimanual manipulation tasks-traditionally performed using a dual-arm manipulator-by employing a single manipulator equipped with a specialized end-effector. To replicate the functional capabilities of two arms within a single end-effector, the fingers mounted on the end-effector must provide higher dexterity than conventional parallel grippers. Human hands, for instance, perform grasping by flexion and abduction of the fingers, and the thumb additionally enables opposition to the other fingers, facilitating stable grasping. However, even the human hand has limited ability to rotate the flexion axis of each finger, and thus cannot fully substitute for arm-like manipulation using finger joints alone.

To address this challenge, the proposed design utilizes three actuated joints for each finger to achieve finger articulation, and incorporates a fingertip gripper to grasp objects at the end phalanx. Although constructing each finger with a higher number of degrees of freedom-similar to a 6- or 7-DoF manipulator-is theoretically possible, such a configuration would significantly increase system complexity. Therefore, in this work, we adopt a minimum-DoF design approach, providing sufficient dexterity to reach desired contact configurations in 3D space while maintaining mechanical simplicity.

The proposed end-effector consists of two fingers, as illustrated in ‘[Fig. 2]’. The end-effector is mounted on a UR3

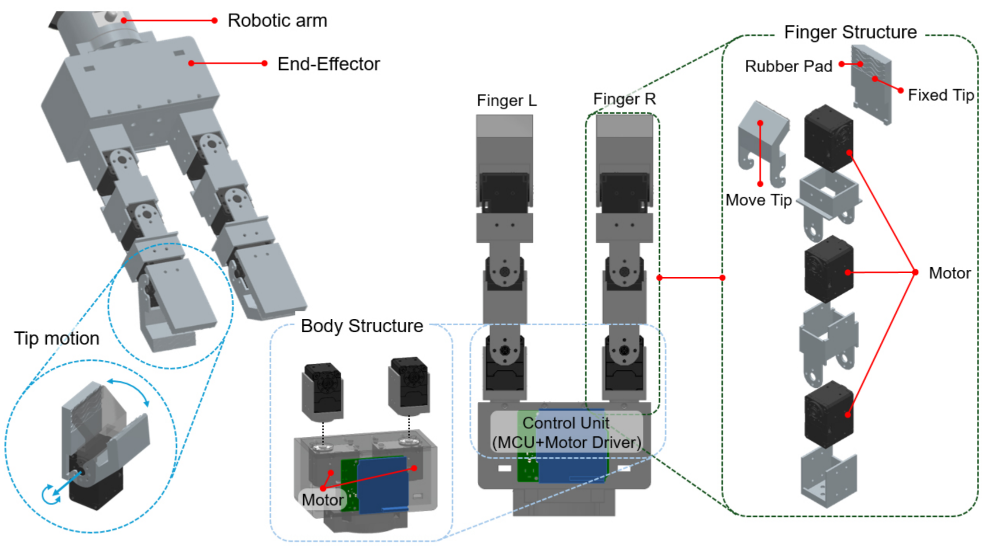

[Fig. 2] Detailed design of the proposed end-effector robot via a customized mechanical adapter integrated into the base structure. Each finger is driven by three rotational joints, with one motor assigned to each joint. The base structure houses the motors responsible for driving the proximal joints of both fingers, along with an onboard MCU and motor drivers. Additional motors are serially mounted along the finger links, and the final motor actuates a compact fingertip gripper. The fingertip consists of a fixed pad attached to the motor frame and a movable pad driven by the motor shaft, enabling secure grasping. Further details on the kinematic structure, motion characteristics, and workspace analysis are presented in the following section.

3.2 Kinematic Analysis

In this section, forward kinematics is performed to describe the motion characteristics of the proposed end-effector. As previously mentioned, each finger is a serial linkage composed of three rotational joints, allowing the position and orientation of the fingertip to be determined. To this end, coordinate frames were assigned to the joints and links, and the forward kinematic model was constructed accordingly. In particular, because each fingertip consists of a fixed tip and a movable tip, these two components are treated separately so that their respective poses can be estimated. Using the derived kinematic model, the fingertip pose and workspace of the fingers are subsequently analyzed.

To describe the behavior of the proposed end-effector, coordinate frames were first assigned to each joint, and the corresponding DH parameters were defined. [Fig. 3] illustrates the coordinate systems of the end-effector ([Fig. 3(a)]) along with its kinematic diagram, while the kinematic parameters are annotated in [Fig. 3(b)].

First, as shown in [Fig. 3(a)], the center of the mounting surface where the manipulator and the gripper are attached is denoted as P_o, and a coordinate frame $P_o x_o y_o z_o$ is assigned such that the direction perpendicular to the surface defines the z_o axis. For the left finger, the analysis proceeds as follows. A coordinate frame $P_{j1} x_1 y_1 z_1$ is attached with its z1 axis aligned with the rotational axis of the first motor. The second and third motors are assigned coordinate frames $P_{j2} x_2 y_2 z_2$ and $P_{j3} x_3 y_3 z_3$, with z_2 and z_3 corresponding to their respective rotational axes. The three points P_{j2}, P_{j3}, and P_{j4} lie along the z_1 axis. Beyond these joints, the fingertip is represented by two terminal points: the

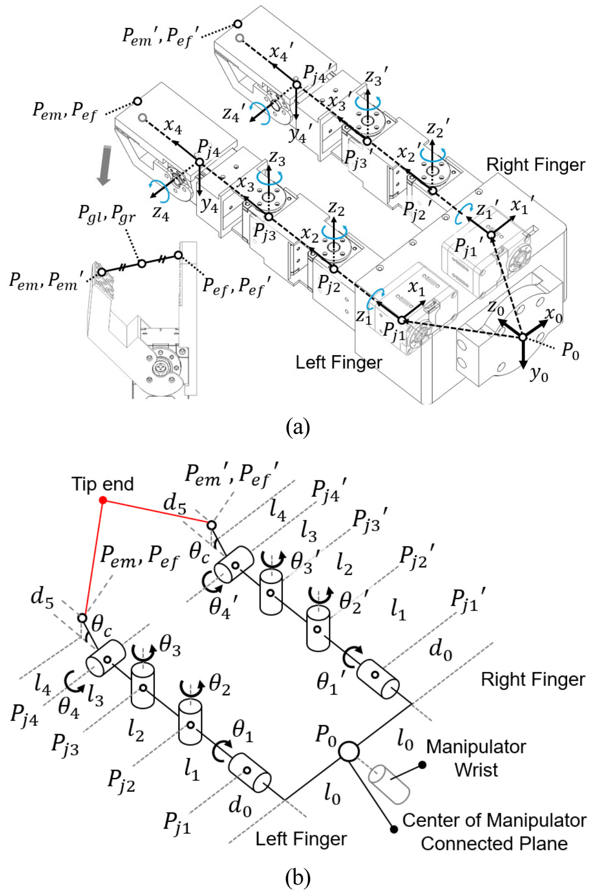

[Fig. 3] Coordinate system and kinematic diagram of the proposed gripper for kinematic analysis, (a) Coordinate System of the end-effector, (b) Kinematic diagram of the end-effector

move tip and the fixed tip, both defined such that their z-axes point toward the object. Since the move tip is actuated by the motor at P_{j4}, the coordinate frame following $P_{j3} x_3 y_3 z_3$ is denoted as $P_{j4} x_4 y_4 z_4$. The end-point of the move tip is labeled as P_{j5}, with its coordinate frame $P_{j5} x_5 y_5 z_5$. In contrast, the fixed tip is unaffected by the motion of the motor at P_{j4} and can therefore be represented as the $P_{j4} x_4 y_4 z_4$ frame when the motor angle satisfies $\theta_4 = 0$.

The right finger has the same coordinate-frame structure as the left finger, except that the signs of the kinematic parameters required for transforming from the base frame $P_o x_o y_o z_o$ to the first motor frame $P_{j1}' x_1' y_1' z_1'$ differ.

[Fig. 3(b)] shows the kinematic diagram constructed based on the coordinate frames defined in [Fig. 3(a)]. The rotational axes of the motors are represented as cylinders, and the notation for all points is kept consistent. The distances between points are denoted as d and l, while the motor rotation angles are variable and labeled as θ_1, θ_2 and θ_3. Finally, the term θ_c annotated at P_{j4} indicates that the endpoint of the move tip does not lie on the z_1 axis in its initial configuration and is affected by θ_4. Consequently, the distance between P_{j4m} and P_{j5m} is $\sqrt{l_4^2+l_5^2}$. The kinematic parameters corresponding to the design dimensions are provided in the appendix.

Let $T_i^j \in SE(3)$ denote the homogeneous transformation matrix from frame i to frame j (where $j > i$). The matrix T_i^j can be expressed as follows.

$$T_i^j = T_i^{i+1} T_{i+1}^{i+2} \cdots T_{j-2}^{j-1} T_{j-1}^j \tag{1}$$

Based on this, and using the coordinate frames defined in [Fig. 3(a)], the transformations from the base frame $P_o x_o y_o z_o$ to $P_4 x_4 y_4 z_4$ can be obtained sequentially as T_0^1, T_1^2, and so on, as follows.

$$T_0^1 = \begin{bmatrix} 1 & 0 & 0 & -l_0 \\ 0 & 1 & 0 & 0 \\ 0 & 0 & 1 & d_0 \\ 0 & 0 & 0 & 1 \end{bmatrix} \tag{2a}$$

$$T_1^2 = \begin{bmatrix} 0 & -\cos\theta_1 & \sin\theta_1 & 0 \\ 0 & -\sin\theta_1 & -\cos\theta_1 & 0 \\ 1 & 0 & 0 & l_1 \\ 1 & 0 & 0 & 1 \end{bmatrix} \tag{2b}$$

$$T_2^3 = \begin{bmatrix} \cos\theta_2 & -\sin\theta_2 & 0 & l_2 \\ \sin\theta_2 & \cos\theta_2 & 0 & 0 \\ 0 & 0 & 1 & 0 \\ 0 & 0 & 0 & 1 \end{bmatrix} \tag{2c}$$

$$T_2^3 = \begin{bmatrix} \cos\theta_3 & 0 & -\sin\theta_3 & l_3 \\ \sin\theta_3 & 0 & \cos\theta_3 & 0 \\ 0 & -1 & 0 & 0 \\ 0 & 0 & 0 & 1 \end{bmatrix} \tag{2d}$$

Here, the coordinates of the move-tip end P_{em} and the fixed-tip end P_{ef}, expressed in the coordinate frame $P_4 x_4 y_4 z_4$, are given as follows.

$$P_{em} = [l_e \cos\theta_{4c} \quad l_e \sin\theta_{4c} \quad 0 \quad 1]^T \tag{3a}$$

$$P_{ef} = [l_e \cos(-\theta_c) \quad l_e \sin\theta_{4c} \quad 0 \quad 1]^T \tag{3b}$$

Here, $\theta_{4c} = \theta_4 - \theta_c$, where θ_4 is the actuation angle of the P_{j4} joint motor, and θ_c is a design parameter. The term $l_e = \sqrt{l_4^2 + l_5^2}$ is also a design parameter.

For the right finger, the same procedure can be applied by replacing $-l_0$ with $+l_0$ in the matrix T_0^1. All coordinate frames and points associated with the right finger are marked with a prime symbol ($'$). Accordingly, the transformation matrix of the right finger is denoted as $T_i^{j'}$, and the transformation from the base frame $P_o x_o y_o z_o$ to the frame $P_4 x_4 y_4 z_4$ is represented as $T_0^{4'}$. The coordinates of the move tip end and the fixed-tip end for the right finger are denoted as P'_{em} and P'_{ef}, respectively.

When an object is grasped using the fixed tip and move tip, it is assumed that the object is held at the midpoint between the two tips. Let the midpoint between the left finger's tips be P_{gl} and that between the right finger's tips be P_{gr}; they are expressed as follows.

$$P_{gl} = \frac{P_{em} + P_{ef}}{2} \tag{4a}$$

$$P_{gr} = \frac{P'_{em} + P'_{ef}}{2} \tag{4b}$$

At this point, if the grasping midpoint of the left finger is expressed in the base coordinate frame $P_o x_o y_o z_o$, the transformed point is denoted as ${}_0P_{gl}$ and is given as follows.

$${}_0P_{gl} = T_0^4 P_{gl} \tag{5}$$

Therefore, the position of the left finger's grasping midpoint P_{gl} expressed in the coordinate frame of the right finger's grasping midpoint P_{gr} is denote as ${}_{gr}P_{gl}$ and is given as follows.

$${}_{gr}P_{gl} = T_0^{4'} T_0^4 P_{gl} \tag{6}$$

Here, the superscript ^{T} in T_i^{jT} denotes the matrix transpose. Finally, in a manner analogous to bimanual manipulation-where the gripper mounted on the left arm is used as the observation frame to express the pose of the gripper mounted on the right arm-the position of the right finger's grasping point can be expressed from the viewpoint of the left finger's grasping point. The kinematic parameters used in this analysis are provided in the appendix.

3.3 Reachable workspace

To achieve a stable grasp, a kinematic analysis of the reachable space of each finger is essential. In particular, for

[Table 1] Joint angle limits of the gripper

Joint angle	Range (degree)
θ_1	-180 to 180
θ_2	-90 to 60
θ_3	-90 to 60
θ_4	0 to 70

structures in which two fingers are equipped with independent grippers, it is important to analyze the workspace of each finger individually and then identify the overlapping region between the two. This overlapping region represents the feasible grasping space in which both fingers can make simultaneous contact with the object, and therefore serves as a key indicator for evaluating the performance of the gripper design.

The motion ranges of each joint and the gripper tips are summarized in [Table 1], and the reachable workspace of each finger was computed based on these ranges. For the grasping midpoints P_{gl} and P_{gr} of the two fingers, all possible positions generated by the combinations of joint angles were plotted to evaluate the overall reachable region. In addition, since the relative position of the grasping midpoint varies depending on the opening width of the tips-which changes according to the size of the object to be grasped-the final reachable region was derived by incorporating this effect as well.

[Fig. 4] illustrates the reachable workspaces of the two fingers in a 3D view as well as top and front views. The left finger is shown in blue and the right finger in red, and the overlapping region of the two colors represents the feasible grasping space in which both fingers can simultaneously reach. Additionally, the overlapping region of the two fingers forms a simultaneous reachable area near the center of the end-effector, representing the spatial range in which both fingers can make contact at the same time. As shown in the top and front views, the two workspaces converge toward each other, which is important because it provides the kinematic allowance for both fingers to reach the same region during grasping. This simultaneous reachable area satisfies the minimum spatial requirement for establishing a grasp on an object. Therefore, the workspace analysis demonstrates that the proposed end-effector possesses sufficient kinematic capability to perform stable two-finger grasping even when mounted on a single manipulator.

In addition, to identify the kinematic characteristics within the overlapping region, the minimum singular value of the Jacobian

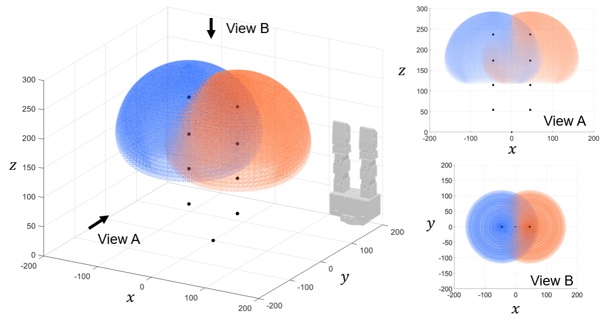

[Fig. 4] Reachable workspace of the end-effector

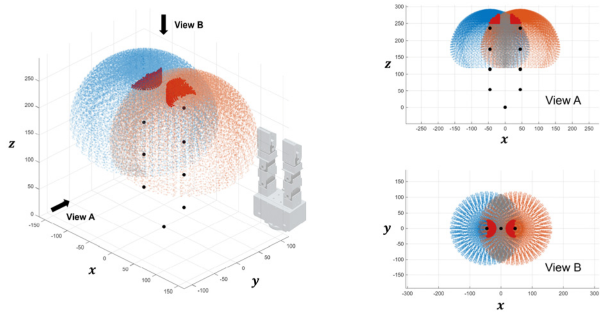

[Fig. 5] Workspace overlap and near-singular regions of both fingers

for each finger was computed, and near-singular regions were visualized. As shown in [Fig. 5], near-singular configurations were identified in certain postures within the overlapping workspace. These configurations correspond to states in which end-effector motions may require large joint velocities, potentially affecting cooperative manipulation stability. Therefore, the experimental trajectories were designed to avoid these regions, and configurations in which both fingers simultaneously approached near-singular states were excluded.

4. Experimental Validation

This section validates the capabilities of the proposed end-effector through three simple bimanual manipulation tasks and one complex bimanual manipulation task. These tasks were selected because they represent the fundamental components of everyday bimanual operations. Prior to the task demonstrations, the gripping force of the gripper and the payload capacity of the non-gripping joints are measured and presented. Based on these experimental results, the functional effectiveness of the proposed end-effector is demonstrated. The configuration of the gripper used in the experiments is described in detail. The gripper consists of a total of seven motors (P_{j1}: XC-430-W230-T, P_{j2} and P_{j3}: XL-430-W250-T, P_{j4}: XM-430-W350-T, Robotis). The motors were controlled using an MCU (Uno, Arduino) and Motor Shield (Dynamicxel Shield, Robotis). The fingers communicate through a daisy chain connection. The end-effector was mounted on a manipulator (UR3, Universal Robot) for use, and its total weight is 0.86 kg.

4.1 Quantitative evaluation

The quantitative evaluation of the end-effector consists of two parts. First, the gripping force generated by the gripper actuated by P_{j4} was measured, and based on this result, the payload capacity of the other joints was evaluated. [Fig. 6(a)] shows the experimental setup for measuring the gripping force. A load cell (QLMH-25, BIRAN) capable of measuring both compression and tension was installed. A connector was attached to the load cell to fasten the wire, and the end-effector grasped a corresponding connector attached to the opposite end of the wire. From this configuration, the manipulator was moved vertically upward to measure the load-cell output, which was used to determine the gripping force. A gravitational acceleration of 9.812 m/s^2 was used for converting the measurement to force, and data were collected at 20 ms intervals over five repeated trials. [Fig. 6(b)] illustrates the resulting force profile over time. The x-axis represents time (s) and the y-axis represents force (N). The five trials are shown in gray, and the averaged result is shown in black. Across five trials, the peak force ranged from 15.14 N to 16.32 N, with an average of 15.77 N.

However, the measured gripping force is a reference value obtained under a specific grasping condition. Since the relative posture of the gripper tips can vary depending on object geometry and contact configuration, the achievable force may differ across different objects. Therefore, this result should be interpreted as an indicative force capability rather than a universal maximum grasping force for all grasping scenarios.

The next evaluation concerns the payload capacity of the manipulator. This measurement was conducted under the same conditions as the gripping force experiment, except that the object was grasped laterally and then lifted vertically upward. [Fig. 7(a)] shows the experimental setup. While the motor driven by P_{j4} operates in current-control mode to ensure gripping stability and prevent overload, the motors in the remaining joints

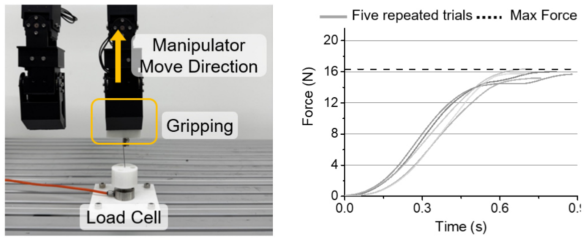

(a) (b)

[Fig. 6] Gripping force evaluation: (a) Measurement setup, (b) Time-domain force response

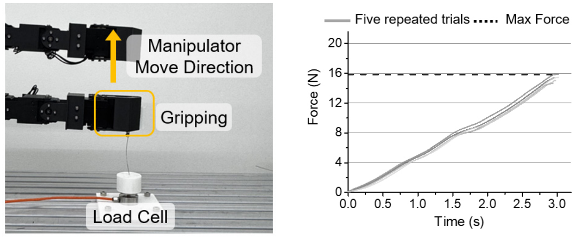

(a) (b)

[Fig. 7] Payload evaluation: (a) Measurement setup, (b) Time-domain force response

operate in position-control mode. Therefore, the load-cell value was recorded up to the point at which an overload was detected in the position-controlled joints. As with the gripping force test, the measurement was repeated five times. The x-axis represents time (s) and the y-axis represents force (N). The five trials are shown in gray, and the averaged result is shown in black. Across five trials, the peak load ranged from 14.59 N to 15.83 N, with an average of 15.42 N.

4.2 Bimanual manipulation

During the bimanual manipulation tasks, the manipulator's actions were executed based on pre-verified teaching positions. Since the purpose of this work is to evaluate the performance of the proposed gripper itself, manipulation tasks and autonomous object search are not considered. The posture for each action is determined beforehand and then applied during the experiments.

First, three simple bimanual manipulation tasks were selected, each consisting of a single primary action. In the context of bimanual manipulation, an action involving direct interaction with an object is defined as a phase. For example, primary actions such as picking or opening require several auxiliary motions, including pose changing, approaching, gripping, and lifting. A phase is thus defined as the sequence of these auxiliary

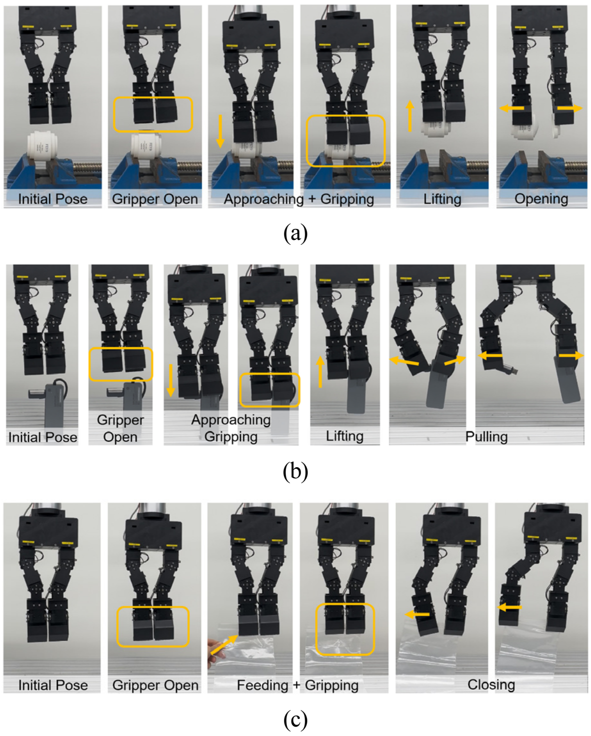

[Fig. 8] Experimental results of three simple bimanual manipulation tasks, (a) Experimental result of opening a container cap, (b) Experimental result of unplugging a USB device, (c) Experimental result of closing a zipper storage bag

motions that collectively enable the primary interaction with the object. Based on this definition, the selected tasks were opening a container cap, unplugging a USB device from a USB hub, and closing a zipper storage bag, whose primary actions correspond to opening, pulling, and closing, respectively.

[Fig. 8] presents the results of the three selected tasks. All tasks begin with the initial pose followed by opening the gripper. The next step involves moving closer to the object: [Fig. 8(a)] and [Fig. 8(b)] correspond to the approaching motion toward the object, while [Fig. 8(c)] shows a feeding motion in which the object is brought toward the end-effector. After this, the object is grasped, and for objects placed on a surface, a lifting motion is performed. Finally, the primary actions-opening, pulling, or closing-are executed to complete the phase. The results of the three single-phase tasks show that each task can be executed with relatively simple motions; however, these actions are inherently difficult to perform with a single hand. Conventional approaches typically require two parallel grippers to execute such tasks. In contrast, the proposed end-effector is capable of completing all three tasks on its own, demonstrating the advantage of the integrated mechanism.

For the complex bimanual manipulation task, a scenario requiring multiple phases was selected. This task involves three primary actions corresponding to unlocking a battery case, opening the case, and retrieving an AA battery from inside. [Fig. 9] illustrates the results of the three-phase experiment.

In the first phase, the gripper moves from the initial pose toward the case, presses one side of the case using one finger, and releases the latch on the other side using another finger. The latch on the opposite side is released in the same manner, after which the gripper changes its pose in preparation for the next phase.

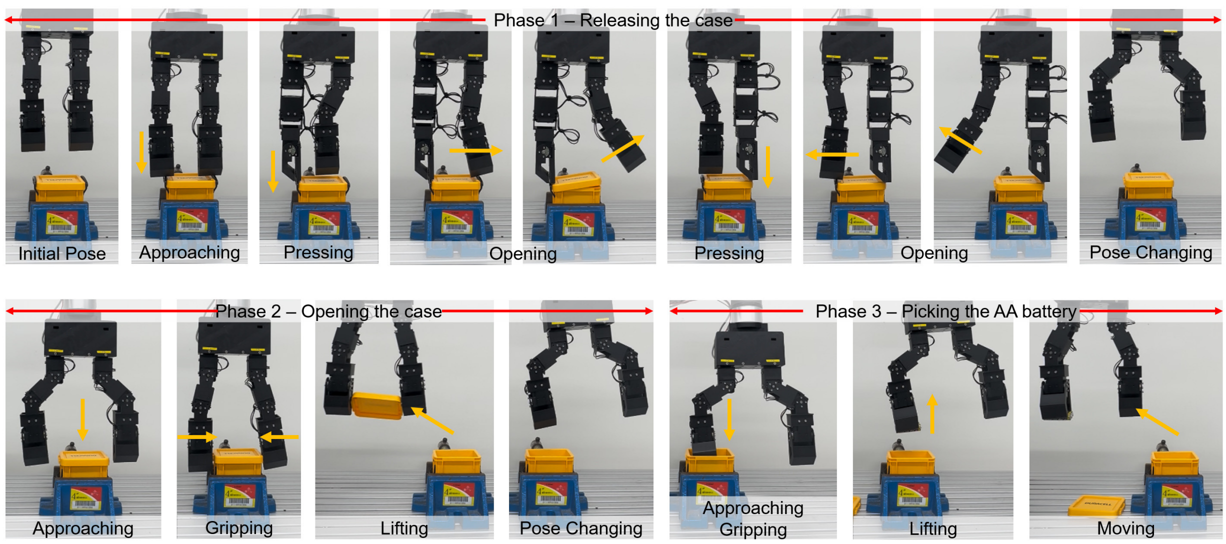

[Fig. 9] Experimental results of three phase complex bimanual manipulation tasks: phase 1 - releasing the case, phase 2 - opening the case, and phase 3 - picking the AA battery

In the second phase, the gripper approaches the case. Since the case is too large to be grasped by a single finger, it is gripped using two fingers. The gripper then lifts the case and performs the opening action, followed by a pose change in preparation for the next phase.

In the third phase, one finger of the gripper is opened and inserted into the interior of the case to grasp the battery. The gripper then lifts and moves the battery outward, completing the picking action.

The results of this three-phase task show that, although each individual action is relatively simple, a substantial number of coordinated motions are required overall. Moreover, the finger movements needed for each action vary significantly, demonstrating that the proposed end-effector is well suited for executing the diverse motions involved in such multi-step manipulation tasks.

4.3 Results

The proposed end-effector generated gripping force and supported payload, both of which were confirmed through experiments without motor overload. Three single-phase manipulation tasks (container opening, USB unplugging, zipper closing) were successfully executed following pre-taught trajectories. A multi-phase task consisting of releasing, opening, and picking steps was also completed using coordinated motion of the two articulated fingers. These experiments confirm that the mechanism can execute diverse manipulation motions using a single manipulator.

5. Discussion

The results of this study demonstrate that the proposed end-effector can reproduce essential bimanual manipulation behaviors even when operated with a single manipulator. Quantitative experiments confirmed that the proposed structure provides sufficient gripping force and payload capacity, and the mechanism successfully performed not only single-phase tasks but also complex multi-phase tasks. Furthermore, the two fingers were shown to exhibit a partially overlapping workspace, and this simultaneous reachable region provides the geometric foundation necessary for forming two contact points with a single end-effector.

The main contributions of this study are as follows. First, we propose an end-effector that enables bimanual manipulation tasks-traditionally requiring two independent grippers or a dual-arm manipulator-to be executed using a single manipulator. By integrating a three-joint articulated finger with a compact fingertip parallel gripper, the mechanism allows a single robot arm to emulate hand–hand coordination. Second, we systematically analyzed the kinematic model and workspace characteristics of the proposed structure, verifying that the overlapping reachable region enables stable dual-sided contact. Finally, through various manipulation scenarios ranging from simple tasks to multi-phase operations, we experimentally demonstrated the practical applicability of the proposed end-effector.

Nevertheless, several limitations remain. The gripping force and payload capacity are suitable only for relatively lightweight objects, and applications requiring high loads-such as those in industrial environments-would require further improvements. Additionally, no external sensor system was integrated, and the mechanism did not use feedback to adapt to environmental variations. As a result, it is difficult for the system to handle object-position uncertainties or unexpected disturbances. Third, although the proposed end-effector can reproduce certain functions of a dual-arm system, it remains limited in tasks that require widely spaced contact points or high torsional torque. Moreover, since the proposed tool combines position-controlled upper joints and a current-controlled fingertip gripper in a serial-link structure, coupling effects may occur due to reaction forces generated during contact. To mitigate this issue, the experiments were conducted under low-speed and limited-acceleration conditions; however, transient vibrations may still appear in tasks involving abrupt contact forces. A systematic dynamic analysis of such coupling effects and feedback-based joint control will be addressed in future work.

In addition, the manipulation trajectories were executed in a teaching-based approach with predefined object poses to validate the mechanical feasibility of the proposed end-effector. The waypoints were manually set by the authors, taking into account the overlapping workspace.

Finally, the proposed end-effector was designed without structural dependency on a specific sensing system. It can be extended in future work by incorporating an RGB-D camera-based vision system to enhance robustness against disturbances.

6. Conclusion

This study presented a new end-effector designed to enable bimanual manipulation using a single manipulator. By integrating a three-joint articulated finger with a fingertip parallel-gripper mechanism, the proposed system demonstrates that actions traditionally requiring a dual-arm setup can be replicated within a single tool. The forward kinematic modeling and workspace analysis confirmed that the mechanism provides the geometric capability needed to generate two simultaneous contact points, and the experimental scenarios verified its functional feasibility across various manipulation tasks.

The primary significance of this work lies in introducing a single-arm manipulation paradigm that can replace certain dual-arm operations while reducing system cost, spatial footprint, and mechanical complexity. This approach has strong potential for application in environments with limited space, mobile or portable robotic platforms, and simplified manipulation systems in industrial or service contexts. Overall, the concept proposed in this study provides a foundation for expanding the functional range of single-manipulator systems and may serve as an enabling technology for future robotic platforms that require compact yet versatile manipulation capabilities.

However, the proposed approach is not intended to fully replace general dual-arm robotic systems. Since the proposed end-effector is implemented at the tool level on a single manipulator, the effective workspace in which practical bimanual manipulation can be achieved is inherently constrained. Tasks that require widely separated contact points, large payloads, or high torsional resistance are therefore better suited to conventional dual-arm robots, which offer a broader workspace and higher mechanical stiffness.

Within its target scope, however, the proposed system is particularly well suited for compact manipulation scenarios where spatial constraints, system weight, or mechanical complexity limit the applicability of dual-arm configurations. By embedding two coordinated contact interfaces into a single end-effector, the proposed mechanism enables functional bimanual-like operations in confined environments, effectively bridging the gap between conventional single-gripper tools and full dual-arm systems. In this sense, the proposed end-effector should be viewed not as a replacement, but as a complementary solution that expands the functional range of single-manipulator platforms.

A. List of Kinematic Parameters

The design dimensions of the kinematic parameters used in the kinematic analysis are listed in ‘[Table 2]’.

[Table 2] List of Mathematical Symbols

Symbol	Values(m)	Description
l_0	45.15	x_0-axis DIS[1] BET[2] P_0 and P_{j1}
l_1	60.25	z_1-axis DIS[1] BET[2] P_{j1} and P_{j2}
l_2	59.25	x_2-axis DIS[1] BET[2] P_{j2} and P_{j3}
l_3	63.25	x_3-axis DIS[1] BET[2] P_{j3} and P_{j4}
l_4	55.00	x_4-axis DIS[1] BET[2] P_{j4} and P_{ef}
d_0	54.20	z_0-axis DIS[1] BET[2] P_0 and P_{j1}
d_5	9.25	$-y_4$-axis DIS[1] BET[2] P_{j4} and P_{ef}

DIS[1]: Distance, BET[2]: Between

References

[1] G. Michalos, K. Dimoulas, K. Mparis, P. Karagiannis, and S. Makris, “A novel pneumatic gripper for in-hand manipulation and feeding of lightweight complex parts—a consumer goods case study,” *The International Journal of Advanced Manufacturing Technology*, vol. 97, no. 9, pp. 3735-3750, DOI: 10.1007/s00170-018-2224-2.

[2] J. Qi, X. Li, Z. Tao, H. Feng, and Y. Fu, “Design and Control of a Hydraulic Driven Robotic Gripper,” *2021 IEEE International Conference on Robotics and Biomimetics (ROBIO)*, Sanya, China, pp. 398-404, 2021, DOI: 10.1109/ROBIO54168.2021.9739260.

[3] T. Takaki and T. Omata, “Grasp Force Magnifying Mechanism for Parallel Jaw Grippers,” *Proceedings 2007 IEEE International Conference on Robotics and Automation*, Rome, Italy, pp. 199-204, 2007, DOI: 10.1109/ROBOT.2007.363787.

[4] D. Roy, “Development of novel magnetic grippers for use in unstructured robotic workspace,” *Robotics and Computer-Integrated Manufacturing*, vol. 35, pp. 16-41, DOI: 10.1016/j.rcim.2015.02.003.

[5] A. Jaiswal and B. Kumar, “VACUUM GRIPPER-AN IMPORTANT MATERIAL HANDLING TOOL,” *International Journal of Science and Technology*, vol. 7, no.1, pp. 1-8, [Online], https://www.semanticscholar.org/paper/VACUUM-GRIPPER-AN-IMPORTANT-MATERIAL-HANDLING-TOOL-Jaiswal-Kumar/6b9a807e44f478c0b7ed0a15cc1b222401601c06.

[6] H. Kang, S. Im, J. Jo, and M.-S. Kang, “Enhancing recycling efficiency: A rapid glass bottle sorting gripper,” *Robotics and Autonomous Systems*, vol. 174, no. 2, pp. 104647, DOI: 10.1016/j.robot.2024.104647.

[7] H. J. Kang, S. H. Yoo, Y. J. Lee, and M.-S. Kang, “Prototype Parallel Gripper Mechanism Equipped with Assisting Grippers for Small Object Grasping and Experimental Validation,” *The*

Journal of Korea Robotics Society, vol. 19, no. 1, pp. 58-64, DOI: 10.7746/jkros.2024.19.1.058.

[8] H. J. Kang, H. J. Kim, I. G. Choi, and M.-S. Kang, "Design and Experimental Validation of Spring-Assisted Two-Finger Parallel Gripper," *2025 25th International Conference on Control, Automation and Systems (ICCAS)*, Incheon, Korea(South), pp. 1-5, 2025, DOI: 10.23919/ICCAS66577.2025.11301143.

[9] K. S. Lee, Y. J. Lee, H. J. Kang, D. I. Park, W. G. Lee, and M.-S. Kang, "Design of Underactuated Three-Finger Gripper for Sorting Small-Sized Electronic Waste," *Transactions of the Korean Society of Mechanical Engineers A,* vol. 48, no. 9, pp. 633-639, DOI: 10.3795/KSME-A.2024.48.9.633.

[10] L. Kang, Y. Yang, J. Yang, and B.-J. Yi, "A Three-Fingered Adaptive Gripper with Multiple Grasping Modes," *2021 IEEE/RSJ International Conference on Intelligent Robots and Systems (IROS)*, Prague, Czech Republic, pp. 6097-6103, 2021, DOI: 10.1109/IROS51168.2021.9636758.

[11] B.-Y. Sun et al., "Design Principle of a Dual-Actuated Robotic Hand With Anthropomorphic Self-Adaptive Grasping and Dexterous Manipulation Abilities," *IEEE Transactions on Robotics*, vol. 38, no. 4, pp. 2322-2340, DOI: 10.1109/TRO.2021.3132532.

[12] U. Kim et al., "Integrated linkage-driven dexterous anthropomorphic robotic hand," *Nature communications*, vol. 12, no. 1, pp. 7177, DOI: 10.1038/s41467-021-27261-0.

[13] C. S. Lovchik and M. A. Diftler, "The Robonaut hand: A dexterous robot hand for space," *Proceedings 1999 IEEE International Conference on Robotics and Automation (Cat. No. 99CH36288C)*, Detroit, MI, USA, pp. 907-912, 1999, DOI: 10.1109/ROBOT.1999.772420.

[14] H. Yang et al., "A low-cost linkage-spring-tendon-integrated compliant anthropomorphic robotic hand: MCR-HAND III," *Mechanism and Machine Theory*, vol. 158, no. 3, pp. 104210, DOI: 10.1016/j.mechmachtheory.2020.104210.

[15] Y. Tlegenov, K. Telegenov, and A. Shintemirov, "An open-source 3d printed underactuated robotic gripper," *2014 IEEE/ASME 10th International Conference on Mechatronic and Embedded Systems and Applications (MESA)*, Senigallia, Itlay, pp. 1-6, 2014, DOI: 10.1109/MESA.2014.6935605.

[16] H. J. Kang, D. H. Han, K. W. Son, and M.-S. Kang, "Design of a reconfigurable three-finger gripper for versatile grasping tasks," *Robotics and Autonomous Systems*, vol. 196, pp. 105264, DOI: 10.1016/j.robot.2025.105264.

[17] B.-Y. Sun et al., "Design Principle of a Dual-Actuated Robotic Hand With Anthropomorphic Self-Adaptive Grasping and Dexterous Manipulation Abilities," *IEEE Transactions on Robotics*, vol. 38, no. 4, pp. 2322-2340, DOI: 10.1109/TRO.2021.3132532.

[18] B. Sundaralingam and T. Hermans, "Relaxed-Rigidity Constraints: In-Grasp Manipulation using Purely Kinematic Trajectory Optimization," *planning*, vol. 6, no. 7, pp. 10-15607, DOI: 10.15607/RSS.2017.XIII.015.

[19] A. Bhatt, A. Sieler, S. Puhlmann, and O. Brock, "Surprisingly Robust In-Hand Manipulation: An Empirical Study," *arXiv: 2201.11503*, 2022, DOI: /10.48550/arXiv.2201.11503.

[20] H. Van Hoof, T. Hermans, G. Neumann, and J. Peters, "Learning robot in-hand manipulation with tactile features," *2015 IEEE-RAS 15th International Conference on Humanoid Robots (Humanoids)*, Seoul, Korea(South), pp. 121-127, 2015, DOI: 10.1109/HUMANOIDS.2015.7363524.

[21] L. Yang et al., "TacGNN: Learning Tactile-Based In-Hand Manipulation With a Blind Robot Using Hierarchical Graph Neural Network," *IEEE Robotics and Automation Letters*, vol. 8, no. 6, pp. 3605-3612, DOI: 10.1109/LRA.2023.3264759.

[22] A. Lee, I. Chuang, L.-Y. Chen, and I. Soltani, "InterACT: Inter-dependency Aware Action Chunking with Hierarchical Attention Transformers for Bimanual Manipulation," *arXiv: 2409.07914*, 2024, DOI: 10.48550/arXiv.2409.07914.

[23] Y. Chen et al., "Towards Human-Level Bimanual Dexterous Manipulation with Reinforcement Learning," *Proceedings of the 36th International Conference on Neural Informational Processing Systems*, New Orleans, LA, USA, pp. 5150-5163, 2022, DOI: 10.48550/arXiv.2206.08686.

[24] T. Asfour, P. Azad, F. Gyarfas, and R. Dillmann, "Imitation Learning of Dual-Arm Manipulation Tasks in Humanoid Robots," *International journal of humanoid robotics*, vol. 5, no. 2, pp. 183-202, DOI: 10.1109/ICHR.2006.321361.

[25] A.-L. Pais Ureche and A. Billard, "Learning Bimanual Coordinated Tasks From Human Demonstrations," *Proceedings of the Tenth Annual ACM/IEEE International Conference on Human-Robot Interaction Extended Abstracts,* Portland, Oregon, USA, pp. 141-142, 2015, DOI: 10.1145/2701973.2702007.

[26] A. X. Lee, H. Lu, A. Gupta, S. Levine, and P. Abbeel, "Learning force-based manipulation of deformable objects from multiple demonstrations," *2015 IEEE International Conference on Robotics and Automation (ICRA)*, Seattle, WA, USA, pp. 177-184, 2015, DOI: 10.1109/ICRA.2015.7138997.

[27] T. Z. Zhao, V. Kumar, S. Levine, and C. Finn, "Learning Fine-Grained Bimanual Manipulation with Low-Cost Hardware," *arXiv:2304.13705*, 2023, DOI: 10.48550/arXiv.2304.13705.

[28] Z. Fu, T. Z. Zhao, and C. Finn, "Mobile ALOHA: Learning Bimanual Mobile Manipulation with Low-Cost Whole-Body Teleoperation," *arXiv:2401.02117*, 2024, DOI: 10.48550/arXiv.2401.02117.

[29] C. Smith et al., "Dual arm manipulation—A survey," *Robotics and Autonomous systems*, vol. 60, no. 10, pp. 1340-1353, DOI: 10.1016/j.robot.2012.07.005.

[30] K. Chu, X. Zhao, C. Weber, M. Li, W. Lu, and S. Wermter, "Large Language Models for Orchestrating Bimanual Robots," *2024 IEEE-RAS 23rd International Conference on Humanoid Robots (Humanoids)*, Nancy, France, pp. 328-334, 2024, DOI: 10.1109/Humanoids58906.2024.10769891.

[31] K. F. Gbagbe, M. A. Cabrera, A. Alabbas, O. Alyunes, A. Lykov, and D. Tsetserukou, "Bi-VLA: Vision-Language-Action Model-Based System for Bimanual Robotic Dexterous Manipulations," *2024 IEEE International Conference on Systems, Man, and Cybernetics (SMC)*, Kuching, Malaysia, pp. 2864-2869, 2024, DOI: 10.48550/arXiv.2405.06039.

[32] I.-C. A. Liu, S. He, D. Seita, and G. Sukhatme, "VoxAct-B: Voxel-Based Acting and Stabilizing Policy for Bimanual Manipulation," *arXiv:2407.04152*, 2024, DOI: 10.48550/arXiv.2407.04152.
[33] M. C. Carrozza, G. Cappiello, S. Micera, B. B. Edin, L. Beccai, and C. Cipriani, "Design of a cybernetic hand for perception and action," *Biological cybernetics*, vol. 95, no. 6, pp. 629-644, DOI: 10.1007/s00422-006-0124-2.
[34] A. Ke, J. Huang, J. Wang, C. Xiong, and J. He, "Optimal design of dexterous prosthetic hand with five-joint thumb and fingertip tactile sensors based on novel precision grasp metric," *Mechanism and Machine Theory*, vol. 171, pp. 104759, DOI: 10.1016/j.mechmachtheory.2022.104759.
[35] H. Liu et al., "Multisensory five-finger dexterous hand: The DLR/HITHand II," *2008 IEEE/RSJ International Conference on Intelligent Robots and Systems*, Nice, France, pp. 3692-3697, 2008,DOI: 10.1109/IROS.2008.4650624.
[36] D. Sharma, K. Tokas, A. Puri, and K. Sharda, "Shadow Hand," *Journal of Advance Research in Applied Science (ISSN: 2208-2352)*, vol. 1, no. 1, pp. 4-7, DOI: 10.53555/nnas.v1i1.692.

강 효 재

2020 한양대학교 ERICA 로봇공학과(학사)
2022~현재 한양대학교 융합로봇시스템학과 석박사통합과정

관심분야: Gripper, Grasping, Robot mechanism design, Art and entertainment robot, and their applications

김 희 준

2023~현재 한양대학교 ERICA 스마트융합공학부 학사 재학

관심분야: Gripper, Grasping, Robot mechanism design

강 민 성

1997 홍익대학교 기계공학과(학사)
2002 홍익대학교 기계공학과(석사)
2013 한양대학교 메카트로닉스학과(박사)
2013~현재 한양대학교 부교수

관심분야: Robot manipulator control, Robot mechanism design, Autonomous mobile robot, Construction robot, Computer vision, and their applications